

Received:
22 November 2017

Revised:
20 January 2018

Accepted:
01 March 2018

<https://doi.org/bjr.20170889>

Cite this article as:

Park S, Yoon J-K, Chung N-S, Kim SH, Hwang J, Lee HY, et al. Correlations between intravoxel incoherent motion diffusion-weighted MR imaging parameters and ^{18}F -FDG PET/CT metabolic parameters in patients with vertebral bone metastases: initial experience. *Br J Radiol* 2018; **91**: 20170889.

FULL PAPER

Correlations between intravoxel incoherent motion diffusion-weighted MR imaging parameters and ^{18}F -FDG PET/CT metabolic parameters in patients with vertebral bone metastases: initial experience

^{1,2}SUNGHOO PARK, MD, ³JOON-KEE YOON, MD, PhD, ⁴NAM-SU CHUNG, MD, ⁵SANG HYUN KIM, MD, ⁶JINWOO HWANG, PhD, ^{7,8}HYUN YOUNG LEE, PhD and ^{1,2}KYU-SUNG KWACK, MD, PhD

¹Department of Radiology, Ajou University School of Medicine, Suwon, South Korea

²Musculoskeletal Imaging Laboratory, Ajou University Medical Center, Suwon, South Korea

³Department of Nuclear Medicine and Molecular Imaging, Suwon, South Korea

⁴Department of Orthopaedic Surgery, Ajou University School of Medicine, Suwon, South Korea

⁵Department of Neurosurgery, Ajou University School of Medicine, Suwon, South Korea

⁶Department of Clinical Science, Philips Healthcare, Seoul, South Korea

⁷Regional Clinical Trial Center, Ajou University Medical Center, Suwon, South Korea

⁸Department of Biostatistics, Yonsei University College of Medicine, Seoul, South Korea

Address correspondence to: Prof Kyu-Sung Kwack
E-mail: xenoguma@gmail.com

Objective: To investigate the relationship between intravoxel incoherent motion (IVIM) diffusion-weighted MRI (DW MRI) parameters and ^{18}F -fluorodeoxyglucose (FDG) (PET/CT) metabolic parameters in patients with vertebral bone metastases.

Methods: 19 patients with vertebral bone metastases were retrospectively included in this institutional review board-approved study. All patients underwent IVIM DW-MRI and ^{18}F -FDG PET/CT before treatment. The IVIM parameters [molecular diffusion coefficient (D), perfusion fraction (f), and perfusion-related D (D^*)] and apparent diffusion coefficient were acquired using 11 b -values (0, 10, 15, 20, 25, 50, 80, 120, 200, 300, and 800 s mm^{-2}). Maximum and mean standardized uptake values (SUVmax and SUVmean, respectively), metabolic tumor volume, and total lesion glycolysis derived from ^{18}F -FDG PET/CT were calculated using thresholds of 3.0 SUV. The associations among parameters were evaluated by Spearman's correlation analysis.

Results: A total of 19 patients and 41 regions of interest were included in this study. The IVIM parameter f was positively correlated with the metabolic parameters SUVmean and SUVmax [$\rho = 0.499$ ($\rho < 0.01$) and $\rho = 0.413$ ($\rho < 0.01$), respectively]. There was a weak positive correlation between D^* and SUVmean ($\rho = 0.321$, $\rho = 0.041$).

Conclusion: IVIM perfusion-related parameters, especially f , were correlated with ^{18}F -FDG PET/CT metabolic parameters in patients with vertebral bone metastases. IVIM DW-MRI, used to evaluate metabolic activity, appears to have diagnostic potential for bone metastasis and may also have utility in monitoring the post-treatment response.

Advances in knowledge: The use of IVIM for vertebral bone metastasis is demonstrated. f may be more suitable to reflect the metabolic activity and may facilitate another diagnostic potential for monitoring the post-treatment response.

INTRODUCTION

The oncological applications of diffusion-weighted MRI (DW-MRI) are rapidly expanding to include detection and monitoring of malignant lesions and metastases.¹ DW-MRI, which does not use ionizing radiation or any tracers, and affords a better spatial resolution, appears promising for the management of breast, prostate, liver, and thyroid cancers, as well as lymphomas.^{1,2} Recently, more advanced MRI

techniques using diffusion, intravoxel incoherent motion (IVIM) DW-MRI have been employed with increasing frequency in the clinic to evaluate tissue perfusion without the use of contrast agents. IVIM DW-MRI is currently used widely to characterize various diseases.^{1,3-5} MRI is also an excellent noninvasive modality for evaluating bone marrow lesions. However, the diffusion characteristics of bone marrow are different from those of other organs because

of the abundant fat tissue in marrow.^{1,6,7} Knowledge regarding the correlations between IVIM parameters and PET metabolic parameters may be beneficial for monitoring the metabolic activity and treatment response of oncology patients. Therefore, the purpose of this study was to explore the relationship between IVIM parameters and PET metabolic parameters in patients with vertebral bone metastases.

METHODS AND MATERIALS

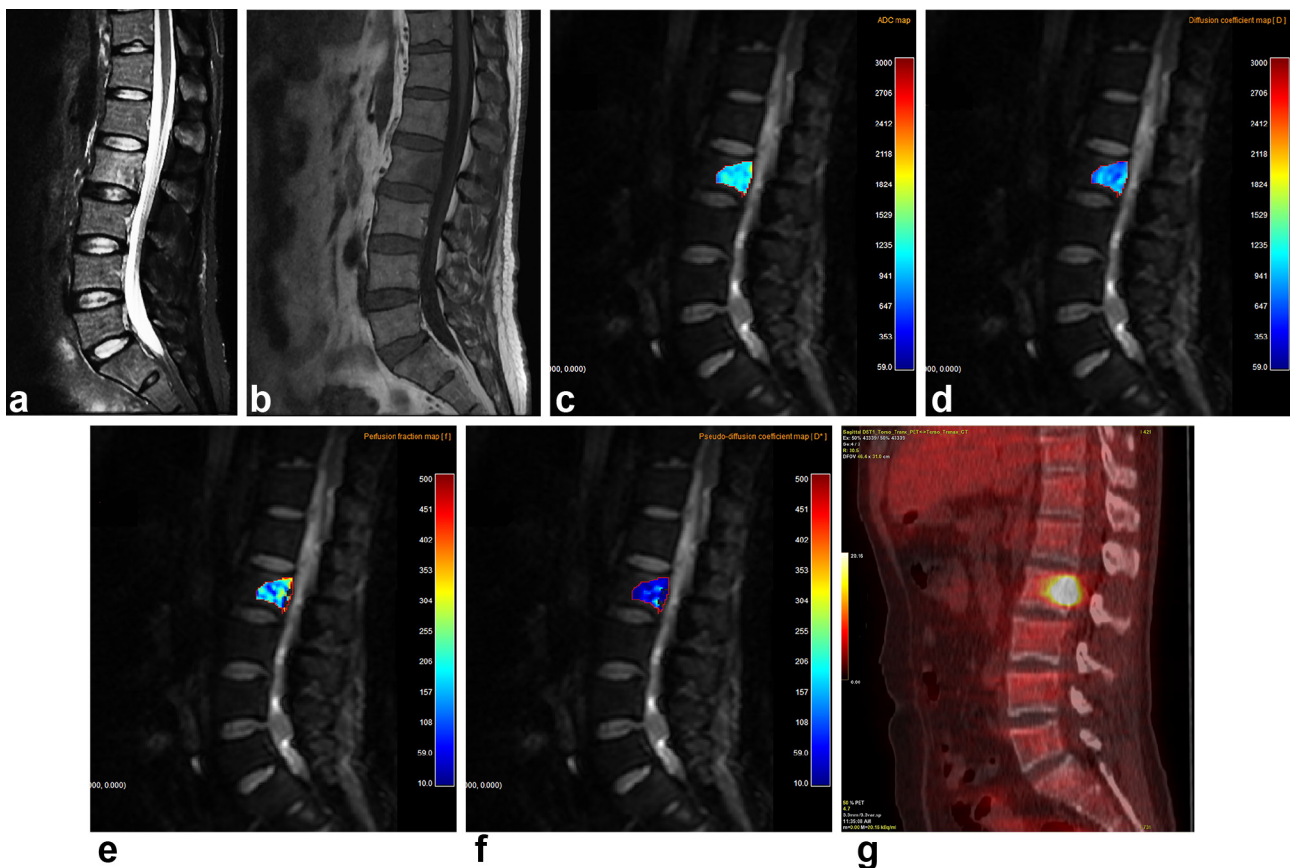
This retrospective study was approved by our institutional review board, and the requirement for written informed consent was waived. We performed a retrospective picture archiving and communication system database search, from April 2015 to August 2016, for all patients registered in the radiology information system who were between 25 and 80 years old and had a clinical history of vertebral bone metastasis. The inclusion criteria available were thoracolumbar or lumbar MRI, IVIM and ¹⁸F-FDG PET/CT scans, performed for initial staging, obtained within 1 month of an evaluation for bone metastases. A total of 79 patients were selected from the picture archiving and communication system database. The exclusion criteria were a lesion less than 1 cm in diameter, unsatisfactory image quality or an

artifact caused by a metal device, a prior history of radiotherapy or chemotherapy, lack of a confirmed diagnosis, and bone metastases accompanied by pathological fractures. On the basis of these inclusion and exclusion criteria, 19 patients were finally included in this study.

Magnetic resonance imaging protocol

All spinal MR examinations were performed using one of two 3.0 T MRI systems (Achieva; Philips Healthcare, Best, Netherlands) with the following parameters (Figure 1): sagittal fat-suppressed T_2 weighted turbo spin echo MRI [repetition time/echo time (TR/TE), 2800/70; echo train length (ETL), 12; section thickness, 3.5 mm; matrix, 512 × 512; field of view (FOV), 300 × 300 mm); sagittal T_1 weighted turbo spin echo MRI (TR/TE, 500/10; ETL, 3; section thickness, 3.5 mm; matrix, 512 × 512; FOV, 300 × 300 mm); axial T_2 -weighted turbo spin echo MRI (TR/TE, 3,500/100; ETL, 15; section thickness, 3.5 mm; matrix, 512 × 512; FOV, 180 × 180 mm); and axial T_1 weighted turbo spin echo MRI (TR/TE, 650/10; ETL, 3; section thickness, 3.5 mm; matrix, 512 × 512; FOV, 180 × 180 mm). IVIM DW-MRI using two-dimensional single-shot diffusion echo planar imaging with 11

Figure 1. A 51-year-old male with biopsy-proven bone metastasis from lung cancer. (a) Sagittal fat-saturated T_2 weighted MR image shows heterogeneous high signal intensity in the lesion at the L2 vertebral body. (b) The mass shown in (a) exhibits heterogeneous low signal intensity on a sagittal T_1 weighted MR image. (c-f) Corresponding ADC (c) and color-coded intravoxel incoherent motion (IVIM) diffusion-weighted MR image-derived molecular diffusion coefficient (D) (d), perfusion fraction (f) (e), and perfusion related- D (D^*) (f) maps are shown. (g) FDG PET/CT shows a hot spot in the L2 vertebral body. ADC, apparent diffusion coefficient; FDG, ¹⁸F-fluorodeoxyglucose; IVIM, intravoxel incoherent motion.



b -values (0, 10, 15, 20, 25, 50, 80, 120, 200, 300, 800 s mm⁻²) was performed in the sagittal plane using the following parameters: TR/TE, 2500/70 ms; ETL, 67; section thickness, 5 mm; matrix, 256 × 256; FOV, 340 × 340 mm; imaging time, 5 min 34 s. Spectral pre-saturation with inversion recovery was applied for fat saturation.

IVIM postprocessing and image analysis

IVIM imaging data were analyzed using in-house IVIM analysis software written in C++ (Visual Studio 2013 Community Edition; Microsoft, Redmond, WA) featuring nonlinear least-squares curve-fitting based on the Levenberg–Marquardt algorithm. The values of apparent diffusion coefficient (ADC) maps were obtained from diffusion-weighted images generated using two b -values (0 and 800 s mm⁻²), assuming that a mono-exponential signal shape conformed to the equation $S_b/S_0 = \exp(-bADC)$, where S_b is the mean signal intensity at a given b -value, and S_0 is the signal intensity observed in the absence of a diffusion gradient. In the IVIM model, the relationship between signal variation and the various b factors is expressed by the following equation⁸: $S_b/S_0 = (1-f) \cdot \exp(-bD) + f \cdot \exp[-b(D + D^*)]$, where f is the fraction of diffusion linked to microcirculation, D is the diffusion parameter representing pure molecular diffusion, and D^* is the perfusion parameter representing incoherent microcirculation within the voxel. D^* is pseudodiffusion (perfusion-related D). As previously reported,^{8,9} the equation can be simplified, and D estimated, using only b -values greater than 200 s mm⁻² with a simple linear equation, as follows: $S_b/S_0 = \exp(-bD)$. Using the D -values determined by the equation,

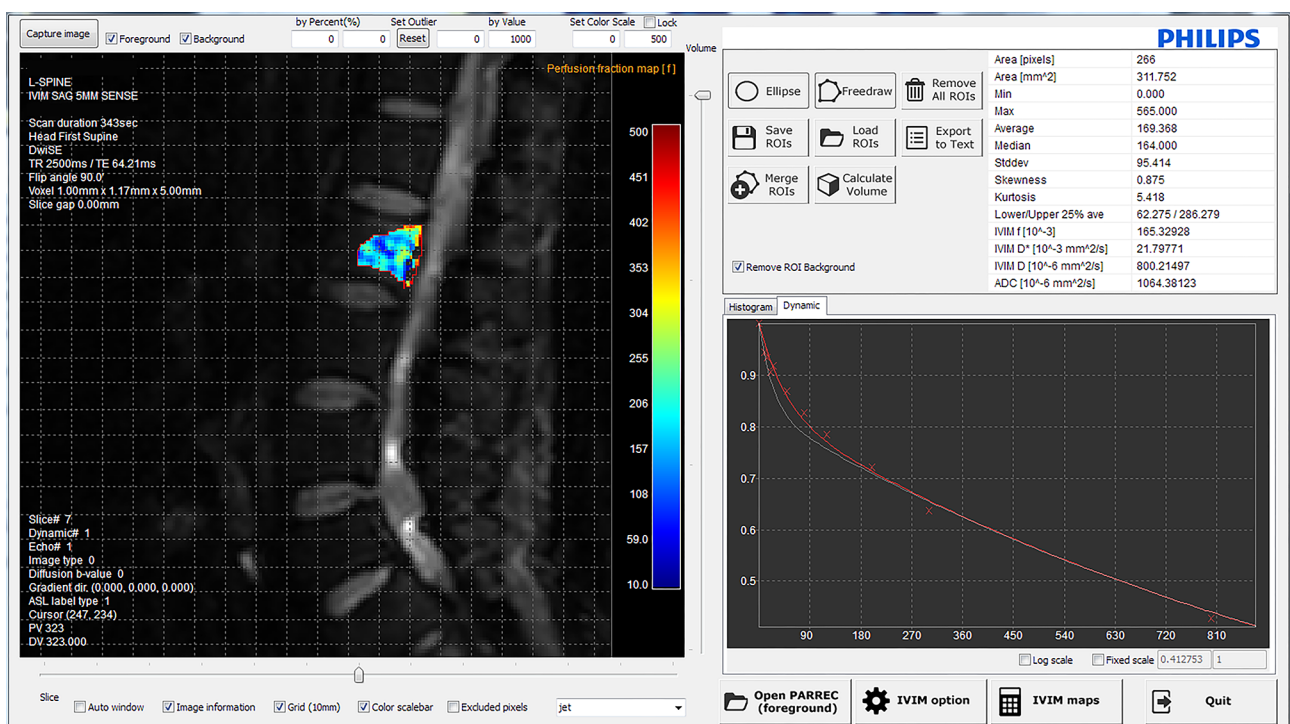
both f - and D^* -values can be calculated by employing a nonlinear regression algorithm (based on the equation).

Quantitative analyses of IVIM DW-MRI were performed by one radiologist (12 years of experience) who was blinded to the patients' information. Diffusion-weighted images (b_0 images) and T_1 weighted images were used to confirm lesion locations and sizes when IVIM DW-MRI were evaluated. Regions of interest (ROIs) were drawn manually on each lesion in the section exhibiting the maximum lesion area (Figure 2). The aim was to cover the most internal part of the lesion while excluding adjacent normal bone marrow. The ROIs were transferred to all multiparametric, IVIM diffusion-weighted maps to minimize potential misalignment. To minimize the potential statistical influence of multiple similar lesions in individual patients with numerous focal vertebral lesions, ROIs were identified for the three largest lesions only of each patient. All ROIs were directly colocalized on all parameter maps. Another radiologist (with 7 years of experience) repeated the ROI measurements to assess interobserver agreement.

¹⁸F-FDG PET/CT protocol

¹⁸F-FDG PET/CT images were obtained using the Discovery ST or STE PET/CT scanner (GE Healthcare, Milwaukee, WI). Patients fasted for at least 6 h and were asked not to perform strenuous exercise for 1 day before the examination. Approximately, 370 MBq ¹⁸F-FDG was injected intravenously into patients with a blood glucose concentration less than 150 mg dl⁻¹. All patients were instructed to rest comfortably for 60 min and to

Figure 2. Graphical user interface of the IVIM analysis software. The ROI was positioned on diffusion-weighted MR images (b₀ images) using in-house IVIM analysis software that automatically calculates IVIM-derived parameters. The graph shows the IVIM signal decay curves of the ROI at the L2 vertebral body. IVIM, intravoxel incoherent motion; ROI, region of interest; TE, echo time; TR, repetition time.



urinate prior to scanning. At first, noncontrast CT images were acquired from the skull base to upper thigh using the following parameters: 120 kV, 60 mA, 7.5 mm per rotation, 1 s per rev tube rotation time, 867 mm scan length, and 60.9 s acquisition time. Immediately after CT scanning, seven to eight frames (3 min per frame) of PET emission data were acquired in the three-dimensional mode. PET emission images were reconstructed using an iterative method (ordered-subsets expectation maximization with two iterations and 30 subsets; FOV = 600 mm, slice thickness = 3.27 mm) and were attenuation corrected by reference to the noncontrast CT image. For quantitation, the patient's body weight and the injected dose were used to calculate the standardized uptake value (SUV; g ml^{-1}).

^{18}F -FDG PET/CT analysis

An experienced nuclear medicine specialist reviewed the images and measured the PET parameters of the vertebral bone marrow lesions that were correlated with those of the spinal MRI. Volumetric metabolic parameters were measured on attenuation-corrected transaxial images using a dedicated workstation (GE Advantage Workstation v. 4.4; GE Healthcare, Milwaukee, WI). The volumetric ROIs (VOIs) were placed carefully over the spinal lesion exhibiting elevated FDG activity (relative to normal tissue) to avoid overlap with adjacent FDG-avid structures and areas exhibiting physiological uptake. The volume viewer software used on a dedicated workstation provided an automatically delineated volume of interest using an isocontour threshold method based on SUV. The maximum SUV (SUVmax), mean SUV (SUVmean), and metabolic tumor volume (MTV) were automatically calculated by the workstation from the VOIs. To define the boundaries of the lesions, a fixed SUV (SUV = 3) was used. Total lesion glycolysis (TLG) was calculated by multiplying the SUVmean by the MTV of the vertebral bone marrow lesions.

Statistical analysis

Means and standard deviations (SDs) were determined for all IVIM and PET/CT vertebral bone metastasis parameters. Spearman's correlation coefficient was used to assess the relationship between PET/CT metabolic parameters (SUVmax, SUVmean, MTV, and TLG) and IVIM parameters (ADC, D , f , and D^*). The degree of correlation was classified according to the correlation coefficient value (ρ) as follows: $0 \leq \rho < 0.2$, weak or no relationship; $0.2 \leq \rho < 0.4$, weak correlation; $0.4 \leq \rho < 0.6$, moderate correlation; $0.6 \leq \rho < 0.8$, strong correlation; and $0.8 \leq \rho$, very strong correlation.^{10,11} Interobserver agreement was quantified by the intraclass correlation coefficient (r). The r -values were classified as follows: 1.0, perfect agreement; 0.81–0.99, almost perfect agreement; 0.61–0.80, substantial agreement; 0.41–0.60, moderate agreement; 0.21–0.40, fair agreement; and ≤ 0.20 , slight agreement.¹² Statistical analyses were performed using the SPSS (v. 22.0; IBM Corp., Armonk, NY) and MedCalc software packages (v. 16.0; MedCalc, Ostend, Belgium). For all assessments, a p value < 0.05 was taken to indicate statistical significance.

RESULTS

A total of 19 patients (8 males, 11 females; mean age, 60.8 ± 10.7 years; range: 40–78 years) and 41 ROI were included in this study. The types of vertebral bone metastasis are summarized

Table 1. Vertebral bone metastases data (number of ROIs) from the various types of histologically confirmed primary cancers

Cancer type	No. of patients	No. of ROIs
Lung cancer	7	16
Breast cancer	4	7
Gastric cancer	2	6
Colorectal cancer	2	4
Renal cell carcinoma	2	4
Ureter cancer	1	3
Cancer of unknown primary site	1	1
Total	19	41

ROI, region of interest.

in Table 1. The primary malignancies of the patients were as follows: lung cancer ($n = 7$), breast cancer ($n = 4$), renal cell carcinoma ($n = 2$), stomach cancer ($n = 2$), colorectal cancer ($n = 2$), ureter cancer ($n = 1$), and cancer of unknown primary site ($n = 1$) (Table 1). The means and SDs of each parameter are summarized in Table 2.

The correlations among ADC, D , f , D^* , SUVmax, SUVmean, MTV, and TLG are summarized in Table 3. Spearman's ρ correlation analysis revealed moderate positive correlations between f and two metabolic parameters (SUVmean and SUVmax; $\rho = 0.499$ and 0.413 respectively, $p < 0.01$) (Figure 3). D^* showed a weak positive correlation with SUVmean ($\rho = 0.321$, $p = 0.041$). No significant relationship was evident between any of the other IVIM parameters and PET metabolic parameters (Table 3).

The intraclass correlation coefficients (r) of the ADC, D , f and D^* values between the two radiologists were 0.967 [95% confidence

Table 2. Mean values of intravoxel incoherent motion diffusion-weighted MR imaging parameters and ^{18}F -fluorodeoxyglucose PET metabolic parameters

	Parameter	Mean \pm SD
MRI	ADC ($\times 10^{-3} \text{ mm}^2 \text{ s}^{-1}$)	0.888 ± 0.289
	D ($\times 10^{-3} \text{ mm}^2 \text{ s}^{-1}$)	0.746 ± 0.280
	f (%)	11.02 ± 5.57
	D^* ($\times 10^{-3} \text{ mm}^2 \text{ s}^{-1}$)	70 ± 287.1
PET	SUVmax	7.1 ± 2.9
	SUVmean	4.2 ± 0.9
	MTV	11.2 ± 11.2
	TLG	50.3 ± 52.9
Total no. of ROIs		41

ADC, apparent diffusion coefficient; D^* , perfusion related- D ; f , perfusion fraction; MRI, magnetic resonance imaging; MTV, metabolic tumor volume; ROI, region of interest; SUVmax, maximum standardized uptake value (SUV); SUVmean, mean SUV; TLG, total lesion glycolysis.

Table 3. Spearman's rho correlations between ¹⁸F-fluorodeoxyglucose PET metabolic parameters and intravoxel incoherent motion diffusion-weighted MRI parameters

		ADC	D	f	D*
SUVmax	Correlation coefficient (ρ)	-0.125	-0.237	0.413 ^a	0.229
	p-value	0.437	0.136	0.007	0.150
	n	41	41	41	41
SUVmean	Correlation coefficient (ρ)	-0.106	-0.226	0.499 ^a	0.321 ^a
	p-value	0.511	0.155	0.001	0.041
	n	41	41	41	41
MTV	Correlation coefficient (ρ)	0.124	0.060	0.090	-0.092
	p-value	0.441	0.709	0.574	0.567
	n	41	41	41	41
TLG	Correlation coefficient (ρ)	0.075	-0.013	0.199	-0.040
	p-value	0.641	0.935	0.211	0.806
	n	41	41	41	41

ADC, apparent diffusion coefficient; D*, perfusion related-D; f, perfusion fraction; MTV, metabolic tumor volume; SUVmax, maximum standardized uptake value (SUV); SUVmean, mean SUV; TLG, total lesion glycolysis.

Weak or no relationship, $0 \leq \rho < 0.2$; weak correlation, $0.2 \leq \rho < 0.4$; moderate correlation, $0.4 \leq \rho < 0.6$; strong correlation, $0.6 \leq \rho < 0.8$; very strong correlation, $\rho \geq 0.8$.

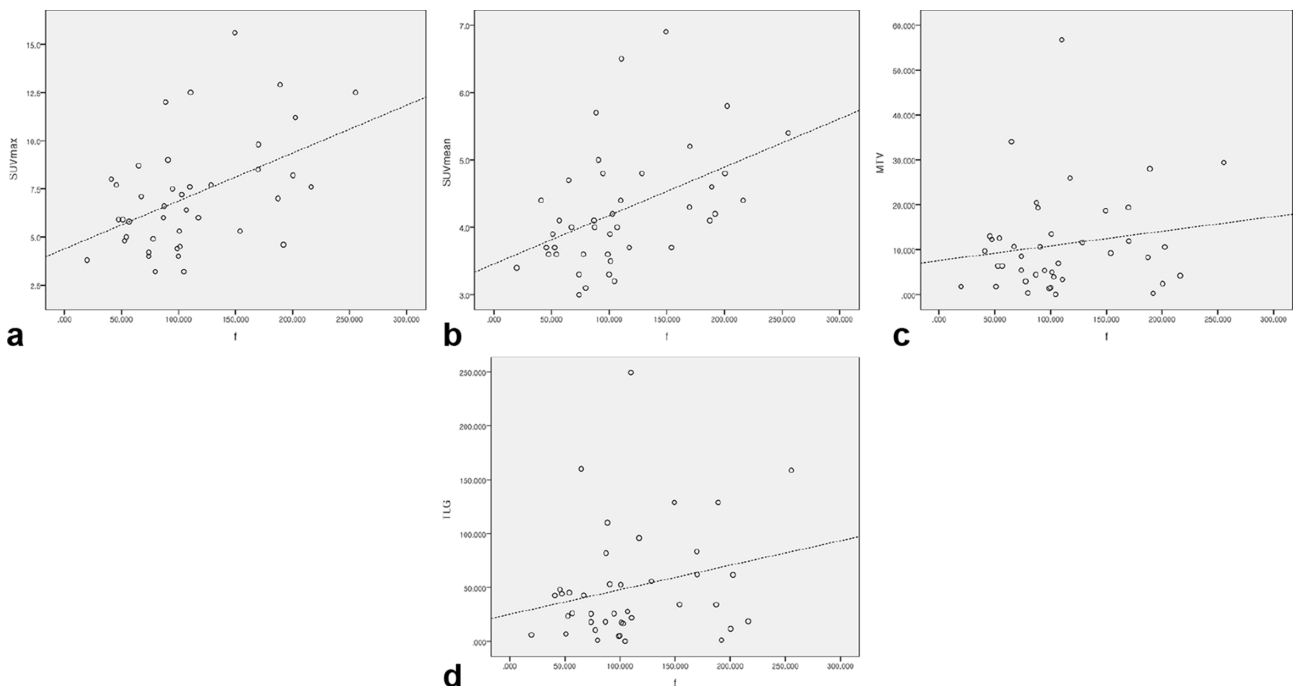
^aCorrelation is significant at the 0.05 level (two-tailed).

interval (CI) (0.938–0.982); $p < 0.001$], 0.972 [95% CI (0.948–0.985); $p < 0.001$], 0.941 [95% CI (0.890–0.969); $p < 0.001$] and 0.599 [95% CI (0.247–0.786); $p = 0.002$], respectively. ADC, D and f exhibited almost perfect agreement. D* revealed moderate agreement.

DISCUSSION

The current study suggested a relationship between IVIM DW-MRI parameters and ¹⁸F-FDG PET/CT metabolic parameters in patients with vertebral bone metastases. Bone metastases

Figure 3. Scatterplots of the correlation between the perfusion fraction and ¹⁸F-FDG PET metabolic parameters. (a–d) Graphs show the results of the correlation analysis among the f and SUVmax (a), SUVmean (b), MTV (c), and TLG (d). Dashed lines represent the trend in each graph. f, perfusion fraction; MTV, metabolic tumor volume; SUVmax, maximum standardized uptake value; SUVmean, mean SUV; TLG, total lesion glycolysis.



or vertebral bone metastases are relatively common in oncology patients. DW-MRI, which does not use ionizing radiation or any tracer and affords better spatial resolution, appears promising for the diagnosis and monitoring of breast, prostate, liver, and thyroid cancers, as well as multiple myelomas and lymphomas.^{1,3} Differences between FDG PET and DW-MRI findings should be expected, as the approaches are underpinned by completely different biophysical mechanisms.^{1,8} In comparison, IVIM DW-MRI is a more advanced diffusion MR technology that uses multiple b -values. To our knowledge, this is the first study to evaluate the relationship between IVIM DW-MRI parameters and ¹⁸F-FDG PET/CT metabolic parameters.

Among the IVIM DW-MRI parameters, f is the microvascular volume fraction that represents the fraction of the diffusion linked to microcirculation.^{9,13} Lima et al^{1,9,13} state that f is a measure of the fractional volume of the capillary blood flowing in each voxel. The f -value may correlate with the amount of normal angiogenesis in intact vessels in terms of basement membrane thickness and pericyte coverage; therefore, the f -value may be an indicator of intact vascular permeability.^{1,13}

A few recent studies have reported a positive correlation between PET/CT metabolic parameters and the perfusion parameters of dynamic contrast-enhanced MRI.^{14–16} There have also been reports showing correlations between dynamic contrast-enhanced MRI perfusion-related parameters and IVIM DW-MRI parameters.^{3,4,17,18}

The present study revealed positive moderate correlations between f and two metabolic parameters (SUV_{mean} and SUV_{max}; $\rho = 0.499$ and 0.413 respectively, $p < 0.01$).

f is the fraction of the diffusion linked to microcirculation, D is the diffusion parameter representing pure molecular diffusion (slow component of diffusion), and D^* is the diffusion parameter representing incoherent microcirculation within the voxel (perfusion-related D ; *i.e.* fast component of diffusion).^{3,9} In our study, D was not significantly correlated with

any metabolic parameter; however D^* showed a weak positive correlation with the SUV_{mean} ($\rho = 0.321$, $p = 0.041$) (Table 3).

Wetter and Rakheja reported a significant negative correlation between SUV and ADC using a PET/MRI system.^{19,20} In our study, although the ADC values showed a decreasing trend with an increase in the SUV_{max}, this result was not statistically significant ($\rho = -0.125$, $p = 0.437$) (Table 2).

PET/CT has been used for quantitative studies, which might be useful to predict the therapy response and determine the prognosis. Previous studies have demonstrated the value of PET/CT to monitor the response of bone metastasis to treatment.^{21,22} Diffusion MRI has been investigated as a potential clinical biomarker in oncology to detect malignant lesions and metastases, as well as to monitor therapy.¹ Our study showed positive moderate correlations between the IVIM DW-MRI parameter and ¹⁸F-FDG PET/CT metabolic parameter. Therefore, IVIM DW-MRI has potential use to monitor the post-treatment response of vertebral bone metastasis. Further studies using IVIM DW-MRI are needed to confirm its reliability and mechanism.

Our study had several limitations. First, it was designed as a pilot investigation and was a retrospective analysis. Second, a small number of patients had vertebral bone metastasis due to the restrictive inclusion criteria. Third, patients who had lesions smaller than 1 cm were excluded from the analysis to avoid any partial-volume effects.

In conclusion, our study showed positive moderate correlations between the IVIM DW-MRI f parameter and the metabolic parameters of ¹⁸F-FDG PET/CT. This suggests the potential utility of IVIM DW-MRI in the diagnosis of bone metastasis by allowing evaluation of metabolic activity. IVIM DW-MRI may also be useful for monitoring the posttreatment response. In light of these promising results, further studies on IVIM DW-MRI are needed to confirm its reliability and reproducibility with respect to monitoring disease progression and the response to therapy in patients with vertebral bone metastasis.

REFERENCES

- Iima M, Le Bihan D. Clinical intravoxel incoherent motion and diffusion MR imaging: past, present, and future. *Radiology* 2016; **278**: 13–32. doi: <https://doi.org/10.1148/radiol.2015150244>
- Padhani AR, Liu G, Koh DM, Chenevert TL, Thoeny HC, Takahara T, et al. Diffusion-weighted magnetic resonance imaging as a cancer biomarker: consensus and recommendations. *Neoplasia* 2009; **11**: 102–25. doi: <https://doi.org/10.1593/neo.81328>
- Bourillon C, Rahmouni A, Lin C, Belhadj K, Beaussart P, Vignaud A, et al. Intravoxel incoherent motion diffusion-weighted imaging of multiple myeloma lesions: correlation with whole-body dynamic contrast agent-enhanced MR imaging. *Radiology* 2015; **277**: 773–83. doi: <https://doi.org/10.1148/radiol.2015141728>
- Wang LL, Lin J, Liu K, Chen CZ, Liu H, Lv P, et al. Intravoxel incoherent motion diffusion-weighted MR imaging in differentiation of lung cancer from obstructive lung consolidation: comparison and correlation with pharmacokinetic analysis from dynamic contrast-enhanced MR imaging. *Eur Radiol* 2014; **24**: 1914–22. doi: <https://doi.org/10.1007/s00330-014-3176-z>
- Yamashita K, Hiwatashi A, Togao O, Kikuchi K, Kitamura Y, Mizoguchi M, et al. Diagnostic utility of intravoxel incoherent motion mr imaging in differentiating primary central nervous system lymphoma from glioblastoma multiforme. *J Magn Reson Imaging* 2016; **44**: 1256–61. doi: <https://doi.org/10.1002/jmri.25261>
- Padhani AR, van Ree K, Collins DJ, D'Sa S, Makris A. Assessing the relation between bone marrow signal intensity and apparent diffusion coefficient in diffusion-weighted MRI. *AJR Am J Roentgenol* 2013; **200**: 163–70. doi: <https://doi.org/10.2214/AJR.11.8185>

7. Marchand AJ, Hitti E, Monge F, Saint-Jalmes H, Guillin R, Duvauferrier R, et al. MRI quantification of diffusion and perfusion in bone marrow by intravoxel incoherent motion (IVIM) and non-negative least square (NNLS) analysis. *Magn Reson Imaging* 2014; **32**: 1091–6. doi: <https://doi.org/10.1016/j.mri.2014.07.009>
8. Le Bihan D, Breton E, Lallemand D, Aubin ML, Vignaud J, Laval-Jeantet M. Separation of diffusion and perfusion in intravoxel incoherent motion MR imaging. *Radiology* 1988; **168**: 497–505. doi: <https://doi.org/10.1148/radiology.168.2.3393671>
9. Luciani A, Vignaud A, Cavet M, Nhieu JT, Mallat A, Ruel L, et al. Liver cirrhosis: intravoxel incoherent motion MR imaging--pilot study. *Radiology* 2008; **249**: 891–9. doi: <https://doi.org/10.1148/radiol.2493080080>
10. Grueneisen J, Beiderwellen K, Heusch P, Buderath P, Aktas B, Gratz M, et al. Correlation of standardized uptake value and apparent diffusion coefficient in integrated whole-body PET/MRI of primary and recurrent cervical cancer. *PLoS One* 2014; **9**: e96751. doi: <https://doi.org/10.1371/journal.pone.0096751>
11. Stelzeneder D, Mamisch TC, Kress I, Domayer SE, Werlen S, Bixby SD, et al. Patterns of joint damage seen on MRI in early hip osteoarthritis due to structural hip deformities. *Osteoarthritis Cartilage* 2012; **20**: 661–9. doi: <https://doi.org/10.1016/j.joca.2012.03.014>
12. Park S, Lee HY, Cuong PM, Won YY, Ji HM, Yoon SH, et al. Supine versus standing radiographs for detecting ischiofemoral impingement: a propensity score-matched analysis. *AJR Am J Roentgenol* 2016; **206**: 1253–63. doi: <https://doi.org/10.2214/AJR.15.15186>
13. Sumi M, Van Cauteren M, Sumi T, Obara M, Ichikawa Y, Nakamura T. Salivary gland tumors: use of intravoxel incoherent motion MR imaging for assessment of diffusion and perfusion for the differentiation of benign from malignant tumors. *Radiology* 2012; **263**: 770–7. doi: <https://doi.org/10.1148/radiol.12111248>
14. Gu J, Khong PL, Wang S, Chan Q, Wu EX, Law W, et al. Dynamic contrast-enhanced MRI of primary rectal cancer: quantitative correlation with positron emission tomography/computed tomography. *J Magn Reson Imaging* 2011; **33**: 340–7. doi: <https://doi.org/10.1002/jmri.22405>
15. Gawlitza M, Purz S, Kubiessa K, Boehm A, Barthel H, Kluge R, et al. *In vivo* correlation of glucose metabolism, cell density and microcirculatory parameters in patients with head and neck cancer: initial results using simultaneous PET/MRI. *PLoS One* 2015; **10**: e0134749. doi: <https://doi.org/10.1371/journal.pone.0134749>
16. Ahearn TS, Staff RT, Redpath TW, Semple SI. The effects of renal variation upon measurements of perfusion and leakage volume in breast tumours. *Phys Med Biol* 2004; **49**: 2041–51. doi: <https://doi.org/10.1088/0031-9155/49/10/014>
17. Liu C, Wang K, Chan Q, Liu Z, Zhang J, He H, et al. Intravoxel incoherent motion MR imaging for breast lesions: comparison and correlation with pharmacokinetic evaluation from dynamic contrast-enhanced MR imaging. *Eur Radiol* 2016; **26**: 3888–98. doi: <https://doi.org/10.1007/s00330-016-4241-6>
18. Jia QJ, Zhang SX, Chen WB, Liang L, Zhou ZG, Qiu QH, et al. Initial experience of correlating parameters of intravoxel incoherent motion and dynamic contrast-enhanced magnetic resonance imaging at 3.0 T in nasopharyngeal carcinoma. *Eur Radiol* 2014; **24**: 3076–87. doi: <https://doi.org/10.1007/s00330-014-3343-2>
19. Wetter A, Lipponer C, Nensa F, Heusch P, Rübber H, Schlosser TW, et al. Quantitative evaluation of bone metastases from prostate cancer with simultaneous [¹⁸F] choline PET/MRI: combined SUV and ADC analysis. *Ann Nucl Med* 2014; **28**: 405–10. doi: <https://doi.org/10.1007/s12149-014-0825-x>
20. Rakheja R, Chandarana H, DeMello L, Jackson K, Geppert C, Faul D, et al. Correlation between standardized uptake value and apparent diffusion coefficient of neoplastic lesions evaluated with whole-body simultaneous hybrid PET/MRI. *AJR Am J Roentgenol* 2013; **201**: 1115–9. doi: <https://doi.org/10.2214/AJR.13.11304>
21. Tateishi U, Gamez C, Dawood S, Yeung HW, Cristofanilli M, Macapinlac HA. Bone metastases in patients with metastatic breast cancer: morphologic and metabolic monitoring of response to systemic therapy with integrated PET/CT. *Radiology* 2008; **247**: 189–96. doi: <https://doi.org/10.1148/radiol.2471070567>
22. Mortazavi-Jehanno N, Giraudet AL, Champion L, Lerebours F, Le Stanc E, Edeline V, et al. Assessment of response to endocrine therapy using FDG PET/CT in metastatic breast cancer: a pilot study. *Eur J Nucl Med Mol Imaging* 2012; **39**: 450–60. doi: <https://doi.org/10.1007/s00259-011-1981-z>